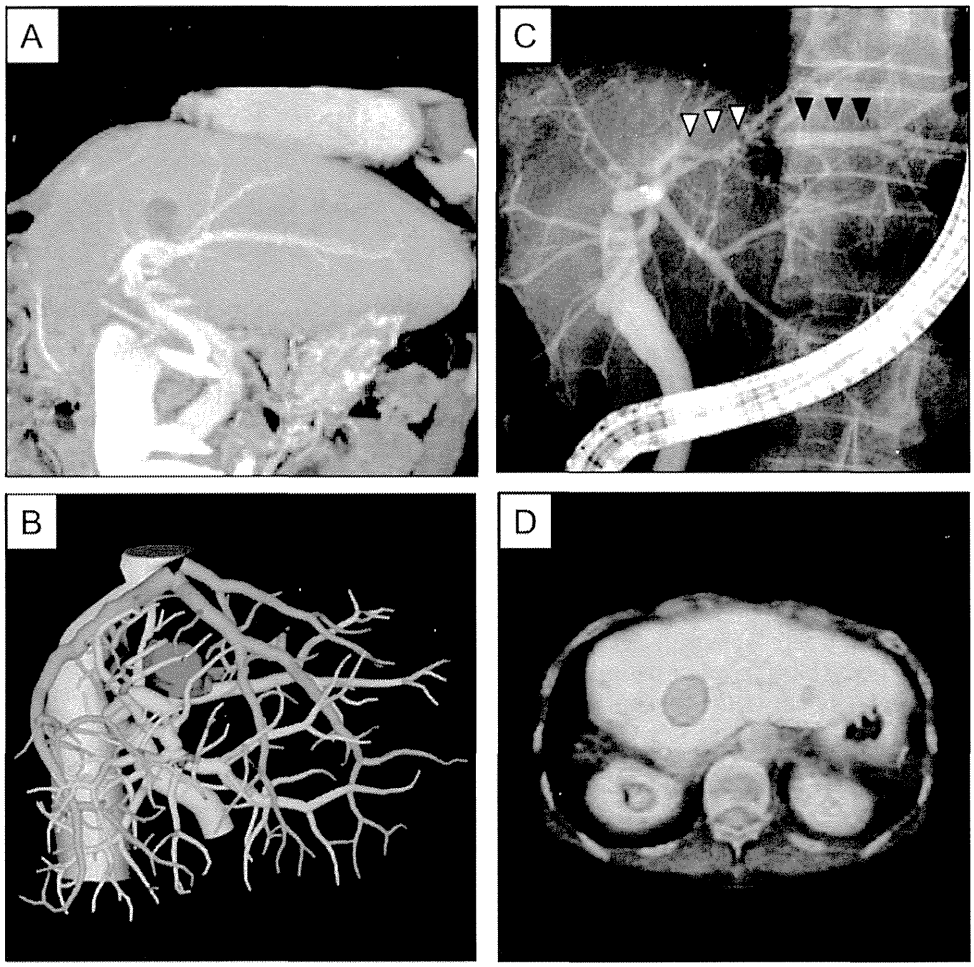

Figure. 1. Preoperative image findings for the de novo liver tumor in the graft. (A,B) Enhanced CT and 3-dimensional CT revealed that the tumor was located just above the umbilical portion. (C) Endoscopic retrograde cholangiography findings. The white and black arrowheads indicate the biliary stricture caused by the tumor and the distal bile duct dilation, respectively. (D) ^{18}F-fluorodeoxy glucose positron emission tomography findings.

Zen et al.[4] suggested that hepatic IPTs could be classified as lymphoplasmacytic or fibrohistiocytic on the basis of the results of immunoglobulin G4 (IgG4) immunohistochemistry. They reported that lymphoplasmacytic IPTs were associated with IgG4-related diseases. In contrast, the pathogenesis of the fibrohistiocytic type remained speculative, but it could represent the end stage of a heterogeneous and destructive inflammatory process. The lymphoplasmacytic IPTs showed some similarities to hepatic malignant lymphoma,[5] a posttransplant lymphoproliferative disorder. Notably, lymphoplasmacytic IPTs were more frequent in patients with Epstein-Barr virus mismatch, excess immunosuppression, and muromonab-CD3 exposure.[1] Our patient had none of these risk factors, and the pathological analyses indicated that the IPT was the fibrohistiocytic type.

Here we have reported the first case of a de novo IPT occurring in a liver graft after LDLT. This case suggests that an IPT could be considered in the differential diagnosis of a de novo liver tumor after LDLT. The prognosis of an IPT is good with or without hepatectomy. Detailed clinical examinations, including biopsy, are important if the preoperative diagnosis is unclear.

Shohei Yoshiya, M.D.[1]
Toru Ikegami, M.D.[1]
Tomoharu Yoshizumi, M.D.[1]
Huanlin Wang, M.D.[1,2]
Noboru Harada, M.D.[1]
Yo-Ichi Yamashita, M.D.[1]
Akihiro Nishie, M.D.[3]
Ken Shirabe, M.D.[1]
Yoshinao Oda, M.D.[2]
Yoshihiko Maehara, M.D.[1]
Departments of [1]Surgery and Science, [2]Anatomic Pathology, and [3]Clinical Radiology
Graduate School of Medical Sciences
Kyushu University
Fukuoka, Japan

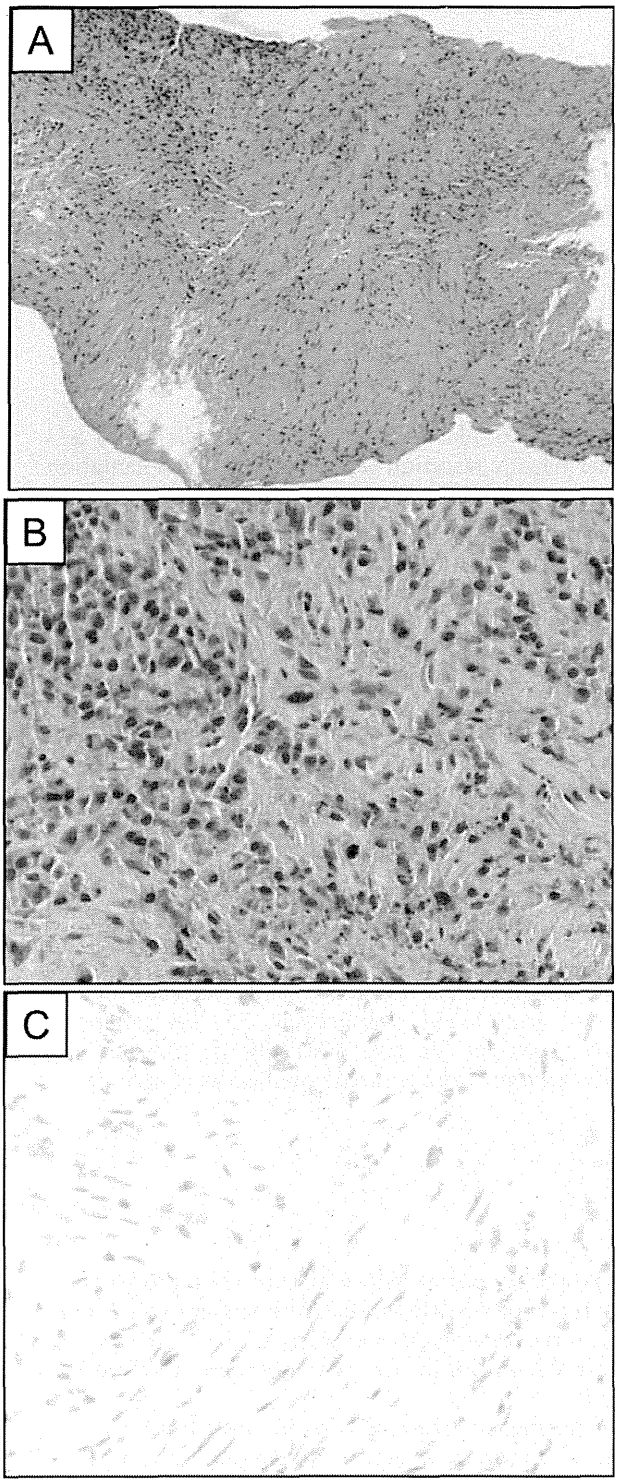

Figure. 2. Pathological analyses of the liver biopsy sample. (A,B) Hematoxylin and eosin staining revealed that the inflammatory lesion was necrotic with a neutrophilic infiltrate, focal fibroblastic proliferation, and lymphoplasmacytic infiltrate. There was no evidence of neoplastic tissue. (C) Immunohistochemically, the plasma cells were negative for IgG4 [original magnification: (A) ×100 and (B,C) ×400].

REFERENCES

1. Chandok N, Watt KD. Burden of de novo malignancy in the liver transplant recipient. Liver Transpl 2012;18: 1277-1289.
2. Horiuchi R, Uchida T, Kojima T, Shikata T. Inflammatory pseudotumor of the liver. Clinicopathologic study and review of the literature. Cancer 1990;65:1583-1590.
3. Ahn KS, Kang KJ, Kim YH, Lim TJ, Jung HR, Kang YN, Kwon JH. Inflammatory pseudotumors mimicking intrahepatic cholangiocarcinoma of the liver; IgG4-positivity and its clinical significance. J Hepatobiliary Pancreat Sci 2012;19:405-412.
4. Zen Y, Fujii T, Sato Y, Masuda S, Nakanuma Y. Pathological classification of hepatic inflammatory pseudotumor with respect to IgG4-related disease. Mod Pathol 2007; 20:884-894.
5. Pecorella I, Ciardi A, Memeo L, Trombetta G, de Quarto A, de Simone P, di Tondo U. Inflammatory pseudotumour of the liver—evidence for malignant transformation. Pathol Res Pract 1999;195:115-120.

Liver INTERNATIONAL
OFFICIAL JOURNAL OF THE INTERNATIONAL ASSOCIATION FOR THE STUDY OF THE LIVER

Liver International ISSN 1478-3223

LIVER CANCER

New scoring system for prediction of microvascular invasion in patients with hepatocellular carcinoma

Ken Shirabe[1], Takeo Toshima[1], Koichi Kimura[1], Yoichi Yamashita[1], Tetsuo Ikeda[1], Toru Ikegami[1], Tomoharu Yoshizumi[1], Koichiro Abe[2], Shinichi Aishima[3] and Yoshihiko Maehara[1]

1 Department of Surgery and Science, Graduate School of Medical Sciences, Kyushu University, Fukuoka, Japan
2 Clinical Radiology, Graduate School of Medical Sciences, Kyushu University, Fukuoka, Japan
3 Anatomic Pathology, Graduate School of Medical Sciences, Kyushu University, Fukuoka, Japan

Keywords
hepatocellular carcinoma – microvascular invasion – prediction – scoring system

Abbreviations
CT, computed tomography; DCP, des-gamma-car boxy prothrombin; FDG-PET, 2-[18F]-fluoro-2-deoxy-D-glucose positron emission tomography; HCC, hepatocellular carcinoma; HR, hepatic resection; LT, liver transplantation; mvi, microvascular invasion; ROC, receiver operating characteristic; SUVmax, maximum standardized uptake value.

Correspondence
Ken Shirabe, MD, PhD, Department of Surgery and Sciences, Graduate School of Medical Sciences, Kyushu University, 3-1-1 Maidashi, Higashi-ku, Fukuoka 812-8582, Japan
Tel: +81-92-642-5466
Fax: +81-92-642-5482
e-mail: kshirabe@surg2.med.kyushu-u.ac.jp

Received 2 August 2013
Accepted 24 December 2013

DOI:10.1111/liv.12459
Liver Int. 2014: 34: 937–941

Abstract

Background & Aims: The microvascular invasion of cancer cells (mvi) is a good prognostic factor after hepatic resection (HR) and liver transplantation for hepatocellular carcinoma (HCC). This study aimed to predict mvi in patients with HCC. *Methods:* We studied 63 hepatectomized patients with HCC who had HCC without any extrahepatic metastases and vascular invasion, which were detected during preoperative evaluation. The preoperative clinicopathological data of these patients were analysed to predict presence of mvi. A scoring system was designed using significant risk factors. This system was applied to another series of 34 patients with HCC who underwent HR, and was evaluated for validation. *Results:* Tumour size, serum des-gamma-carboxy prothrombin (DCP) levels and the maximum standardized uptake value (SUVmax) on 2-[18F]-fluoro-2-deoxy-D-glucose positron emission tomography were independent clinical predictors for mvi after multivariate analyses. Tumour size, serum DCP levels, and values of SUVmax were used to plot a receiver operating characteristic curve for predicting mvi. Areas under the curve of tumour size, serum DCP levels and SUV max values, were 0.8652, 0.8027 and 0.7848 respectively. Maximal sensitivity and specificity were obtained when the tumour size was 3.6 cm, SUVmax was 4.2, and the serum DCP level was 101 mAU/ml. A scoring system was designed using these three variables. The sensitivity and specificity of our scoring system were 100% and 90.9%, respectively, in the validation test. *Conclusion:* Our scoring system for mvi, consisting of tumour size, serum DCP levels, and SUV max, provides a precise prediction of mvi.

Vascular invasion is a major determinant of outcome after hepatic resection (HR) and liver transplantation (LT) in patients with hepatocellular carcinoma (HCC) (1, 2). In patients treated with HR and LT, evidence suggests that not only macrovascular invasion, but microvascular invasion (mvi), is a major determent of outcome in most studies. According to a systematic review, the presence of mvi affects disease-free survival at 3 (relative risk = 1.82) and 5 years (relative risk = 1.51) after HR. After LT, the presence of mvi shortens disease-free survival at 3 years (relative risk = 3.41) and overall survival at 3 (relative risk = 2.41) and 5 years (relative risk = 2.29) (3).

Although magnetic resonance imaging and ultrasonography can detect tumour thrombus in major branches of the portal vein or hepatic veins, the presence of mvi cannot be diagnosed before surgery (4). Therefore, precise preoperative prediction of the presence of mvi would be helpful for patient selection before HR and LT.

We previously proposed a scoring system, which consisted of tumour size, serum des-gamma-carboxy prothrombin (DCP) levels and histological tumour differentiation (5). Our previous scoring system provided precise predictions of the presence of mvi. Nevertheless, tumour biopsy was necessary for the evaluation of histological differentiation of cancer cells. In some candidates for LT with decompensated liver function, tumour biopsy is a contraindication for the risk of intra-abdominal bleeding.

In HCC, the maximum standardized uptake values (SUVmax) on 2-[18F]-fluoro-2-deoxy-D-glucose positron emission tomography (FDG-PET) have been reported to be a useful diagnostic tool for the preoperative evaluation of histological differentiation of cancer cells (6, 7).

Therefore, in the current study, we proposed a new scoring system to predict the presence of mvi, using quantitative factors.

Patients and methods

Patients

Between April 2010 and March 2013, 88 patients who underwent HR and nine living related donor LTs for HCC at Kyushu University Hospital were enrolled in this study. In the first 63 patients, independent risk factors for mvi were examined. In 34 patients who later underwent HR, the resected specimens were examined to warrant the accuracy of our scoring system.

Methods

The following variables were examined: age and gender of the patients, Child–Pugh score, tumour size, tumour number, serum alpha fetoprotein (AFP) and DCP levels, and SUVmax on FDG-PET. Measurements of serum DCP levels were described previously (5).

^{18}F-FDG PET/computed tomography (CT)

2-[18F]-fluoro-2-deoxy-D-glucose positron emission tomography studies were performed with Discovery ST Elite (GE Healthcare, Milwaukee, WI, USA) and Biograph mCT (Siemens AG, Erlangen, Germany) PET/CT scanners. All patients fasted for at least 4 h before FDG administration, and 185 MBq of FDG was intravenously administered to each patient. Approximately 60 min after the FDG injection, whole-body PET images were acquired from thigh to head with 7–10 bed positions. The Discovery ST Elite scanner consists of a 16-slice multidetector CT and bismuth germanate crystal. Unenhanced CT was performed first with the following parameters: 5-mm slice thickness, 120 kV, and 30–250 mAs with auto mode (Smart mA; GE Healthcare, Waukesha, WI, USA). PET images were then obtained in 3D mode for three minutes per bed position with a 3.27-mm slice thickness, at 70 cm field of view in a 128 × 128 matrix. Based on the CT data, transmission maps were created and used for attenuation correction of the PET images. The PET data were reconstructed using a 3D ordered subsets expectation maximization algorithm (VUE Point Plus; GE Healthcare) with two iterations and 28 ordered subsets. A six-millimeter postfilter of full-width at half maximum was applied. The Biograph mCT scanner was equipped with a 128-slice multidetector CT and lutetium oxyorthosilicate crystal. Unenhanced CT was performed at 120 kV with automatic mAs adjustment (Care Dose 4D; Siemens Healthcare, Malvern, PA, USA) and the slice thickness was 3 mm. The PET emission time was 2 min per bed position. The PET images were acquired with a 2-mm slice thickness, at 70 cm field of view in a 256 × 256 matrix. The concomitant CT data were used for attenuation correction. The PET data were reconstructed using a 3D ordered subsets expectation maximization algorithm with two iterations and 21 subsets. Time of flight and point spread function techniques were also used for image reconstruction (ultra HD-PET; Siemens Healthcare). A 3D Gaussian filter of 6-mm full-width at half maximum was applied. The SUVmax values in the tumour were qualitatively evaluated (6).

Histological study

All of the partial hepatectomized specimens and the explanted liver for HCC after living donor LT were cut into 5-mm thick slices and fixed in 10% formalin. After a macroscopic examination, the slice with the greatest dimension and other slices containing areas of possible metastases or mvi were trimmed for paraffin blocks and cut into 4-μm microscopic sections. Sections were then stained with haematoxylin and eosin (H&E). Mvi was considered present when clusters of cancer cells were observed in the portal vein, intracapsular vessels and hepatic vein. We then divided sections into two groups according to mvi: the mvi (+) group and the mvi (−) group. Microscopic examination of these sections was performed by pathologists (Y. M. and S.A.), and a consensus was reached.

Statistical methods

We analysed the associations between continuous and categorical clinicopathological variables and mvi using the Student's *t*-test and chi-square test respectively.

Univariate prediction factors for mvi ($P < 0.05$) were entered into a logistic regression model to identify the independent mvi predictors. Statview software was simultaneously used for the multivariate adjustment of all covariates by means of logistic regression analysis on an IBM computer. In addition, the diagnostic value of liver stiffness for prediction of mvi was assessed by calculating the areas under the receiver operating characteristic (ROC) curves. The ROC curve is a plot of sensitivity vs 1-specificity for all possible cut-off values. A *P* value was considered statistically significant if it was less than 0.05.

Results

Univariate predictors of microvascular invasion

The univariate predictors of mvi were examined in 63 patients (Table 1). Twenty-three patients had mvi (36.5%). Tumour size, preoperative serum DCP levels

Table 1. Clinicopathological background

Factors	mvi(−) (n = 40)	mvi(+) (n = 23)	P-value
Age	65 ± 9	65 ± 14	0.9169
Gender (male/female)	19:21	15:8	0.1995
Child-Pugh score (A:B:C)	35:4:1	18:2:3	0.2552
Tumour size (cm)	2.5 ± 1.3	6.3 ± 4.0	<0.0001
Tumour number (single/multiple)	33/7	19/4	0.999
AFP (ng/ml)	76 ± 177	59158 ± 217389	0.0888
DCP (mAU/ml)	122 ± 331	19775 ± 55263	0.0272
SUVmax	2.7 ± 3.4	9.2 ± 8.5	<0.0001
Histological differentiation (well/moderate/poor)	5/31/4	0/14/9	<0.0001

AFP, alpha fetoprotein; DCP, des-gamma-carboxy prothrombin; SUVmax, the maximum standardized uptake value, mvi, microvascular invasion.

and SUVmax on FDG-PET were statistically significant predictors for mvi. The mean tumour size (cm) in the mvi (−) group was significantly lower than that in the mvi (+) group (2.5 ± 1.3 vs 6.3 ± 4.0, $P < 0.0001$). Preoperative serum DCP (mAU/ml) levels in the mvi (−) group were significantly lower than those in the mvi (+) group (122 ± 331 vs 19775 ± 55263, $P = 0.0272$). SUVmax on FDG-PET in the mvi (−) group was significantly lower than that in the mvi (+) group (2.7 ± 3.4 and 9.2 ± 8.5, $P < 0.0001$). No other factors were significant predictors for mvi.

Independent predictors of microvascular invasion after logistic regression analysis

Univariate predictors ($P < 0.1$) were entered into a logistic regression model to identify the independent predictors of mvi (Table 2). Independent predictors of mvi were tumour size, preoperative DCP levels and SUVmax on FDG-PET. The odds ratios for tumour size, preoperative DCP levels and SUVmax were 2.390, 2.131 and 1.999 respectively.

Determination of cut-off values for tumour size, DCP levels and SUV max using a ROC curve

Tumour size, serum DCP levels and values of SUVmax were used to plot an ROC curve for predicting mvi. The results of the ROC curve are shown in Fig. 1. Areas under the curve of tumour size, serum DCP levels and SUV max values, were 0.8652, 0.8027 and 0.7848 respectively. Maximal sensitivity and specificity were obtained when the tumour size was 3.6 cm, SUVmax was 4.2, and the serum DCP level was 101 mAU/ml.

Scoring system for the prediction of mvi

The frequency distribution of mvi according to tumour size, preoperative serum DCP levels and SUVmax on FDG-PET was examined in the resected specimens of 34 patients who underwent HR for HCC. Mvi was present in none of the patients with a score of less than 2. The percentage of patients who had mvi rose to 90.9% in patients with a score equal to or greater than 2 ($P < 0.0001$). A scoring system was designed using these three variables. The sensitivity and specificity of our scoring system were 100% and 90.9%, respectively, in a validation test.

Discussion

The presence of mvi in HCC is a significant prognostic factor after HR and LT (3). In our study, the incidence of recurrence after curative resection of HCC within 1 year after HR was significantly higher in patients with mvi (+) HCC than in those with mvi (−) HCC (data not shown). Furthermore, the prediction of mvi before treatment of HCC is important. If the presence of mvi is expected, the patient might not be a good candidate for LT, considering the high incidence of HCC recurrence after LT (3). In patients with small HCC and a high risk of mvi, local treatment, such as radiofrequency ablation (RFA) and percutaneous ethanol injection therapy (8), are not recommended as an initial treatment because of a high local recurrence rate. HR may be recommended for prevention of local recurrence, instead of RFA and percutaneous ethanol injection therapy. Ueno *et al.* (9). showed that the effect of anatomical resection was more prominent in the subgroup with nonboundary type nodules (single nodular type with extranodular growth, confluent multinodular type and invasive type) than in the subgroup with the boundary type (vaguely nodular and single nodular type). They found that the incidence of mvi in patients with the nonboundary type of HCC was significantly higher than that in those with the boundary type of HCC. A high incidence of mvi in the

Table 2. Logistic regression for independent predictors for microvascular invasion

Predictor	OR	Regression coefficient	95% CI	SE	P-value
SUVmax	1.999	1.202	1.004–1.440	0.092	0.0456
DCP	2.131	1.002	1.000–1.003	0.001	0.0331
Tumor size	2.390	1.848	1.117–3.059	0.257	0.0168
AFP	0.395	1.001	0.997–1.004	0.002	0.6927

AFP, alpha-fetoprotein; CI, confidence interval; DCP, des-gamma-carboxy prothrombin; OR, odds ratio; SE, standard error; SUVmax, maximum standardized uptake value.

Table 3. Scoring system for the prediction of microvascular invasion

Predictors	Point 0	Point 1
SUVmax	<4.2	≥4.2
DCP (mAU/ml)	<101	≥101
Tumour size (cm)	<3.6	≥3.6

DCP, des-gamma-carboxy prothrombin; SUVmax, maximum standardized uptake value.

Table 4. Prediction of the presence of mvi in another series of 34 patients with HCC who underwent hepatic resection

Presence of mvi	Prediction score for mviScore ≥2	Score <2
(+)	12	0
(−)	2	20

HCC, hepatocellular carcinoma; mvi, microvascular invasion.

nonboundary type of HCC has been reported compared with that in the boundary type of HCC (9–11). This is because anatomical resection is more favourable than non-anatomical resection and RFA in eradicating micrometastasis, including mvi. Therefore, the study by Ueno *et al.* (9). showed that if the presence of mvi is expected, anatomical resection should be used instead of non-anatomical resection and RFA. From this point of view, prediction of mvi is important in determining therapeutic modalities, such as RFA, HR and LT.

In this study, we proposed a new scoring system for the prediction of mvi, using significant predictors of tumour size, serum DCP levels and SUV max on FDG-PET.

In previous studies, several clinicopathological factors have been reported to be predictors for mvi. These factors include tumour size, number, histological differentiation, gross classification of tumours, serum DCP, the value of diffusion-weighted magnetic resonance imaging, portal perfusion defect area on CT during arterioportography and SUVmax on FDG-PET (9–17).

Some reports have shown that serum DCP levels can predict the presence of mvi (12–15). DCP is reported to be a unique tumour marker, reflecting HCC progression. Kim *et al.* (14). showed that elevated DCP levels are closely associated with mvi, even in small HCC. Fujiki *et al.* (15). showed that the incidence of portal vein invasion in patients with high DCP levels >400 mAU/ml, tumour size >5 cm, and a tumour number >10 was significantly higher than in those without these criteria.

2-[18F]-fluoro-2-deoxy-D-glucose positron emission tomography could be a promising tool for prediction of mvi. In a retrospective study, a positive preoperative FDG-PET scan was an independent predictive factor for vascular invasion. Positive and negative predictive values were 87.5% and 88.5% respectively. However, the definition of vascular invasion in this previous study included the involvement of lobar portal vein branches, which is macrovascular invasion (16). Another recent study using dual traces (^{18}FDG and ^{11}C acetate) reported predictive values of 60–64% for FDG-PET in predicting mvi, and this did not improve (^{11}C acetate PET 17). In this study, the cut-off value of SUVmax was determined and this may be related to a better predictive power of FDG-PET scans.

Other modalities, which can be used to determine the presence of mvi, are histological differentiation and gross classification (11, 12, 18, 19). Nevertheless, preoperative diagnosis of histological differentiation and gross classification involves practical problems (11, 20). Tumour biopsy is inevitable for diagnosis of tumour differentiation. Nevertheless, histological variation within a HCC nodule can be so considerable that a single biopsy does not represent the whole tumour. Cabibbo *et al.* (21). stressed the possibility of massive bleeding, but did not touch on the concept that HCC is rarely biopsied because of a rich blood supply and the possibility of the tumour spreading within the peritoneal cavity and along the biopsy needle tract. Hui, *et al.* (11). showed that gross classification of the tumour is related to the incidence of mvi, although it is difficult to obtain an objective diagnosis of gross classification by preoperative CT. Unfortunately, the rate of correct diagnosis for gross classification by preoperative CT is only 46%.

With regard to portal perfusion defects on CT during arterio-portography, our previous study showed that the sensitivity was 58% and specificity was 91% (22). Although the specificity of CT during arterio-portography is high, the sensitivity is relatively low, and the

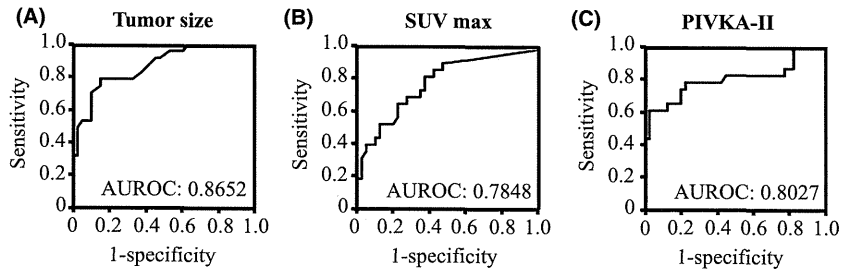

Fig. 1. Receiver operating characteristic (ROC) curves of tumour size, serum DCP levels and values of SUVmax for predicting mvi. The areas under the curve (AUC) of tumour size (1A), serum DCP levels (1B) and SUV max values (1C), were 0.8652, 0.8027 and 0.7848 respectively. DCP, des-gamma-carboxy prothrombin; SUVmax, the maximum standardized uptake value.

discriminative power may be inferior to other diagnostic modalities in precise diagnoses. Nishie *et al.* (23). also reported that in a similar examination, tumour diameter was less than 3 cm, and positive and negative predictive values were 71.4% and 75.0% respectively. They suggested that this discriminative power may not be sufficient for prediction of mvi. Furthermore, this method can be applied to portal vein invasion, but not to hepatic vein invasion.

In the current study, the OR for each factor ranged from 1.999 to 2.390. Therefore, precise prediction for mvi cannot be achieved only by a single parameter. Consequently, a scoring system consisting of three factors is necessary. The present study established a scoring system for prediction of mvi with high discriminative power.

In conclusion, our scoring system consisting of tumour size, DCP levels and SUVmax on FDG-PET provided a precise preoperative diagnosis of the presence of mvi. This scoring system is important for selection of candidates of HR and LT for HCC.

Acknowledgements

Financial support: This research was supported in part by Mitsui Life Social Welfare Foundation.

Conflict of interest: The authors do not have any disclosures to report.

References

1. Ikai I, Arii S, Kojiro M, *et al.* Reevaluation of prognostic factors for survival after liver resection in patients with hepatocellular carcinoma in a Japanese nationwide survey. *Cancer* 2004; **101**: 796–802.
2. Hu Z, Zhou J, Wang H, *et al.* Survival in liver transplant recipients with hepatitis B- or hepatitis C-associated hepatocellular carcinoma: the chinese experience from 1999 to 2010. *PLoS ONE* 2013; **8**: e61620.
3. Rodríguez-Perálvarez M, Luong TV, Andreana L, *et al.* A systematic review of microvascular invasion in hepatocellular carcinoma: diagnostic and prognostic variability. *Ann Surg Oncol* 2013; **20**: 325–39.
4. Chandarana H, Robinson E, Hajdu CH, *et al.* Microvascular invasion in hepatocellular carcinoma: is it predictable with pretransplant MRI? *AJR Am J Roentgenol* 2011; **196**: 1083–9.
5. Shirabe K, Itoh S, Yoshizumi T, *et al.* The predictors of microvascular invasion in candidates for liver transplantation with hepatocellular carcinoma-with special reference to the serum levels of des-gamma-carboxy prothrombin. *J Surg Oncol* 2007; **95**: 235–40.
6. Ijichi H, Shirabe K, Taketomi A, *et al.* Clinical usefulness of (18) F-fluorodeoxyglucose positron emission tomography/computed tomography for patients with primary liver cancer with special reference to rare histological types, hepatocellular carcinoma with sarcomatous change and combined hepatocellular and cholangiocarcinoma. *Hepatol Res* 2013; **43**: 481–7.
7. Khan MA, Combs CS, Brunt EM, *et al.* Positron emission tomography scanning in the evaluation of hepatocellular carcinoma. *J Hepatol* 2000; **32**: 792–7.
8. Ni JY, Xu LF, Sun HL, *et al.* Percutaneous ablation therapy versus surgical resection in the treatment for early-stage hepatocellular carcinoma: a meta-analysis of 21,494 patients. *J Cancer Res Clin Oncol* 2013; **139**: 2021–33.
9. Ueno S, Kubo F, Sakoda M, *et al.* Efficacy of anatomic resection vs nonanatomic resection for small nodular hepatocellular carcinoma based on gross classification. *J Hepatobiliary Pancreat Surg* 2008; **15**: 493–500.
10. Shirabe K, Aishima S, Taketomi A, *et al.* Prognostic importance of the gross classification of hepatocellular carcinoma in living donor-related liver transplantation. *Br J Surg* 2011; **98**: 261–7.
11. Hui AM, Takayama T, Sano K, *et al.* Predictive value of gross classification of hepatocellular carcinoma on recurrence and survival after hepatectomy. *J Hepatol* 2000; **33**: 975–9.
12. Inagaki Y, Tang W, Makuuchi M, *et al.* Clinical and molecular insights into the hepatocellular carcinoma tumour marker des-γ-carboxyprothrombin. *Liver Int* 2011; **31**: 22–35.
13. Yamamoto K, Imamura H, Matsuyama Y, *et al.* AFP, AFP-L3, DCP, and GP73 as markers for monitoring treatment response and recurrence and as surrogate markers of clinicopathological variables of HCC. *J Gastroenterol* 2010; **45**: 1272–82.
14. Kim JM, Hyuck C, Kwon D, *et al.* Protein Induced by Vitamin K Antagonist-II (PIVKA-II) Is a Reliable Prognostic Factor in Small Hepatocellular Carcinoma. *World J Surg* 2013; **37**: 1371–8.
15. Fujiki M, Takada Y, Ogura Y, *et al.* Significance of des-gamma-carboxy prothrombin in selection criteria for living donor liver transplantation for hepatocellular carcinoma. *Am J Transplant* 2009; **9**: 2362–71.
16. Kornberg A, Freesmeyer M, Barthel E, *et al.* 18F-FDG-uptake of hepatocellular carcinoma on PET predicts microvascular tumor invasion in liver transplant patients. *Am J Transpl* 2009; **9**: 592–600.
17. Cheung TT, Chan SC, Ho CL, *et al.* Can positron emission tomography with the dual tracers [11 C]acetate and [18 F] fludeoxyglucose predict microvascular invasion in hepatocellular carcinoma? *Liver Transpl* 2011; **17**: 1218–25.
18. Adachi E, Maeda T, Kajiyama K, *et al.* Factors correlated with portal venous invasion by hepatocellular carcinoma: univariate and multivariate analyses of 232 resected cases without preoperative treatments. *Cancer* 1996; **77**: 2022–31.
19. Sumie S, Kuromatsu R, Okuda K, *et al.* Microvascular invasion in patients with hepatocellular carcinoma and its predictable clinicopathological factors. *Ann Surg Oncol* 2008; **15**: 1375–82.
20. Gouw AS, Balabaud C, Kusano H, *et al.* Markers for microvascular invasion in hepatocellular carcinoma: where do we stand? *Liver Transpl* 2011; **17**(Suppl 2): S72–80.
21. Cabibbo G, Craxì A. Needle track seeding following percutaneous procedures for hepatocellular carcinoma. *World J Hepatol* 2009; **1**: 62–6.
22. Shirabe K, Kajiyama K, Abe T, *et al.* Predictors of microscopic portal vein invasion by hepatocellular carcinoma: measurement of portal perfusion defect area ratio. *J Gastroenterol Hepatol* 2009; **24**: 1431–6.
23. Nishie A, Yoshimitsu K, Asayama Y, *et al.* Radiologic detectability of minute portal venous invasion in hepatocellular carcinoma. *AJR Am J Roentgenol* 2008; **190**: 81–7.

The Apelin–APJ System Induces Tumor Arteriogenesis in Hepatocellular Carcinoma

JUN MUTO[1,4], KEN SHIRABE[1], TOMOHARU YOSHIZUMI[1], TORU IKEGAMI[1], SHINICHI AISHIMA[2], KOUSEI ISHIGAMI[3], YOSHIKAZU YONEMITSU[4], TETSUO IKEDA[1], YUJI SOEJIMA[1] and YOSHIHIKO MAEHARA[1]

Departments of [1]Surgery and Science, [2]Anatomic Pathology, and [3]Clinical Radiology, Graduate School of Medical Sciences, Kyushu University, Fukuoka, Japan; [4]R&D Laboratory for Innovative Biotherapeutics, Graduate School of Pharmaceutical Sciences, Kyushu University, Fukuoka, Japan

Abstract. *Aim: The apelin-APJ system regulates angiogenesis, and is overexpressed in several types of cancer. The aim of this study was to clarify the role of the apelin-APJ system in the angiogenesis of hepatocellular carcinoma (HCC). Materials and Methods: Expressions of angiogenic factors and vascular markers were investigated in specimens from 90 HCC patients. A subcutaneous HCC tumor mouse model was treated with the APJ antagonist, F13A, and tumor growth and vascular development were assessed. Results: APJ expression was observed in arteriole-smooth muscle. Higher amounts of APJ^+-arteriole and apelin were detected in tumors ($p<0.001$ for both). APJ^+-arteriole and apelin expression were more commonly observed in moderately- and poorly-differentiated than in well-differentiated HCC ($p\leq0.003$). HCC with irregular dilated arteries expressed higher levels of apelin ($p=0.012$). Tumor growth was inhibited by treatment with F13A ($p<0.001$), and arterioles were decreased in the treated group ($p=0.047$), in vivo. Conclusion: Apelin-APJ is overexpressed, and works as a signal for arteriogenesis in HCC.*

Abbreviations: Ang-1, Angiopoietin-1; ang-2, angiopoietin-2; AVD, arterial vessel density; CASMC, coronary artery smooth muscle cell; ERK, extracellular signal-regulated kinase; H&E, hematoxylin and eosin; HCC, hepatocellular carcinoma; GAPDH, glyceraldehyde 3-phosphate dehydrogenase; IHC, immunohistochemistry; MAPK, mitogen-activated protein kinase; MEK, MAPK extracellular signal-regulated kinase; MVD, microvessel density; qRT-PCR, quantitative reverse transcriptase-polymerase chain reaction; VEGF, vascular endothelial growth factor.

Correspondence to: Ken Shirabe, Department of Surgery and Science, Graduate School of Medical Sciences, Kyushu University, 3-1-1 Maidashi, Higashi-ku, Fukuoka 812-8582, Japan. Tel: +81 926425466, Fax: +81 926425482, e-mail: kshirabe@surg2.med.kyushu-u.ac.jp

Key Words: Apelin, APJ, hepatocellular carcinoma, arteriogenesis, angiogenesis.

Hepatocellular carcinoma (HCC) is a highly vascular tumor characterized by neoangiogenesis, which contributes to the high rate of metastasis and dismal prognosis (1-5). A recent study by Matsui *et al.* reported that the intranodular portal supply decreases during the early stages of hepatocarcinogenesis, whereas the intranodular arterial supply initially decreases and subsequently increases in parallel with increasing grade of malignancy of the nodules (6). This can be demonstrated using contrast-enhanced computed tomography (CT) scanning or angiography, in which hyperattenuation is observed in the arterial phase and hypoattenuation in the portal phase. Thus, the inhibition of neoangiogenesis represents a promising approach in treating HCC (7). Tumor cells have been widely shown to affect tumor angiogenesis, and several angiogenic proteins have been identified, including vascular endothelial growth factor (VEGF), angiopoietin-1 (ang-1) and angiopoietin-2 (ang-2) (8-10). However, the molecular mechanisms underlying tumor-associated neoangiogenesis in HCC are still unclear.

Apelin, a secreted peptide, was identified as the endogenous ligand of the G-protein-coupled cell-surface apelin receptor (APJ) (11, 12). Apelin and APJ mediate a wide range of physiological actions, including angiogenesis (13, 14), heart contractility (15) and blood pressure regulation (16). Apelin and APJ are expressed on endothelial cells of newly-developing blood vessels during angiogenesis (14). APJ has also been detected on vascular smooth muscle cells and affects proliferation (17). APJ mediates phosphorylation of the myosin light chain (18). Kidoya *et al.* reported apelin-deficient mice to have narrow blood vessels, whereas apelin-overexpressing mice had enlarged blood vessels (19), which were stable, with reduced vascular permeability.

Previous studies have reported that expression of apelin is a poor prognostic factor in both non-small cell lung cancer (20) and oral squamous cell carcinoma (21); overexpression of apelin is also observed in breast cancer (22). Overexpression

0250-7005/2014 $2.00+.40

of apelin was shown to enhance vascularization and encourage tumor growth in murine tumor models (23, 24).

Herein, we analyzed expression and function of the apelin-APJ system in HCC, and examined the therapeutic effects of inhibiting the apelinergic system in a HCC murine tumor model.

Materials and Methods

Human tissue samples. Tissue specimens were obtained from 90 patients who had undergone liver resection for HCC without preoperative treatment, at the Department of Surgery and Science, Kyushu University Hospital, between January 2004 and December 2009. Samples were collected after obtaining informed consent, according to an established protocol approved by the Ethics Committee of the Kyushu University.

Animal model of HCC. Experimental procedures were approved by the Kyushu University Institutional Animal Care and Use Committee and conformed to the guidelines outlined in the Guide for the Care and Use of Laboratory Animals prepared by the National Academy for Sciences and published by the National Institutes of Health.

A previously established subcutaneous HCC mouse model was used (25). Mice were treated with F13A (American Peptide Company, Vista, CA; 2000 μg/kg daily) *via* intraperitoneal injection, and tumor development was monitored.

Immunohistochemistry (IHC) and quantification of angiogenesis. IHC images were scanned using a confocal microscope (Radiance 2100; BioRad) and digitally processed with the Image J software (NIH image), as previously established (26). Images from three marker-positive areas were analyzed. The mean count of three hot spots was used for statistical analysis. All data were analyzed by two pathologists who had no prior knowledge of the clinicopathological findings.

Statistical analysis. Data are expressed as the mean±the standard error of the mean (SEM). Statistical evaluations of numerical variables between different groups were mainly performed using the Mann–Whitney *U*-test. Differences in tumor growth were statistically analyzed using one-way ANOVA. Significant differences were determined by post-hoc Fisher's exact probability test. Differences were considered statistically significant at $p<0.05$. Analyses were performed using JMP (version 8.0.1, SAS, Inc., Cary, NC) or GraphPad Prism 4 software (version 5.0d, GraphPad Software Inc, La Jolla, CA).

Results

Tumor vascularity in patients with HCC. The microvessel density (MVD) was calculated in tissue samples by IHC staining for the vascular endothelial marker, CD34 (Figure 1A). The mean MVD of tumor tissues was 2.1-fold higher than in non-tumor tissues ($p<0.001$) (Figure 1B, left). In addition, the MVD of moderately- and poorly-differentiated HCCs was significantly higher than well-differentiated HCCs ($p=0.020$ and $p=0.012$, respectively; Figure 1B, right). We next investigated the arterial vessel density (AVD) by immunohistochemical analysis of an arterial smooth muscle cell marker, high-molecular-weight caldesmon (h-caldesmon; Figure 1C). AVD was significantly higher in tumors ($p<0.001$; Figure 1D, left), and AVD of moderately- and poorly-differentiated HCCs was also significantly higher than well-differentiated HCCs ($p=0.012$ and $p=0.012$, respectively; Figure 1D, right). APJ expression was also examined (Figure 1E). APJ expression was clearly detected in tumor arteries, and the incidence of APJ^+ vessels was higher in tumors than in non-tumorous tissues ($p<0.001$; Figure 1F, left). Similar to MVD and AVD patterns, APJ^+ arteries were more commonly observed in moderately- and poorly-differentiated HCCs than in well-differentiated HCCs ($p=0.003$ and $p=0.002$, respectively; Figure 1F, right). Co-expression of CD34 with APJ (Figure 1G) was next investigated by double immunohistochemical staining. We observed that APJ was expressed on arterial smooth muscle cells, but not endothelial cells. The incidence of APJ^+ vessels was more strongly correlated with h-caldesmon$^+$ vessels in tumors (r=0.793, $p<0.001$; Figure 1H, right) than in non-tumorous tissues (r=0.251, $p=0.019$; Figure 1H, left).

Expression of angiogenic factors in HCC. We next examined the expression of several key angiogenic factors by qRT-PCR. Expression of *ang-1* was 2.1-fold higher in tumor tissue than in normal liver tissue ($p<0.001$; Figure 2A, left). Although *ang-1* expression did not significantly vary with histological differentiation, there was a trend towards higher expression in moderately- and poorly-differentiated HCCs than in well-differentiated HCCs ($p=0.570$, $p=0.222$, respectively; Figure 2A, right). Similar to *ang-1*, expression of *ang-2* was 2.1-fold higher in tumor tissue ($p<0.001$; Figure 2B, left). Furthermore, expression of *ang-2* was significantly greater in moderately- and poorly-differentiated HCCs ($p=0.005$ and $p=0.003$, respectively; Figure 2B, right). In contrast, we observed no significant difference in *VEGF* expression between tumor and non-tumor specimens ($p=0.707$; Figure 3C, left), and no significant differences could be associated with histological differentiation ($p=0.465$, $p=0.829$; Figure 2C, right). *Apelin* mRNA expression was 5.7-fold higher in tumor than in non-tumorous tissue ($p<0.001$; Figure 2D, left). Expression of apelin was also elevated in moderately- and poorly-differentiated HCCs compared with well-differentiated HCCs ($p=0.002$ and $p=0.002$, respectively; Figure 2D, right).

Angiogenic factors and preoperative radiological images. The ratio of *ang-2* and *ang-1* mRNA (ang-2/ang-1) was shown to be high in tumors with CTHA enhancement ($p=0.039$, Figure 3A, B left), whereas *apelin* mRNA expression was not correlated with tumor enhancement ($p=0.859$; Figure 3B right).

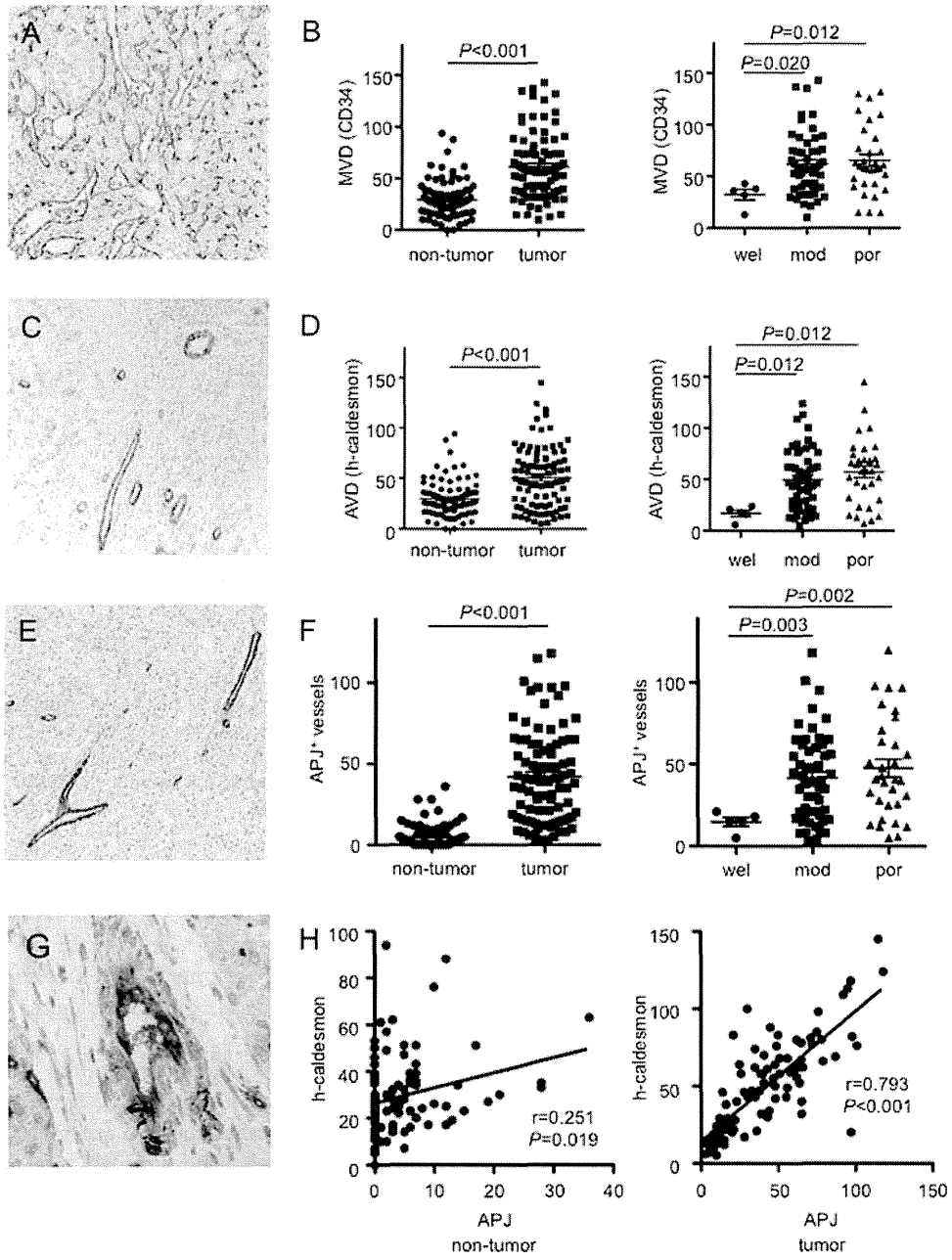

Figure 1. *Neoangiogenesis and APJ expression in HCC. (A) CD34 immunostaining. (B) Mean MVD calculated using CD34 was greater in moderately- and poorly-differentiated HCCs than in well-differentiated HCC (p=0.020, p=0.012, respectively). (C) h-Caldesmon immunostaining. (D) Mean AVD calculated using h-caldesmon was greater in moderately-and poorly-differentiated HCCs than in well-differentiated HCC (p=0.012 and p=0.012, respectively). (E) APJ immunostaining. (F) APJ+ vessels were greater in moderately- and poorly-differentiated HCCs than in well-differentiated HCC (p=0.003 and p=0.002, respectively). (G) CD34 (blue) and APJ (brown) double immunohistostaining. (H) Although APJ and h-caldesmon expression was positively correlated in non-tumor tissue (r=0.251, p=0.019), this correlation was much stronger in HCCs (r=0.793, p<0.001).*

Irregular dilatation of tumor-feeding arteries was also observed by digital subtraction angiography (Figure 3C). Tumors displaying irregular dilated feeding arteries expressed significantly higher levels of apelin than tumors with no feeding artery dilatation (p=0.012; Figure 3D right). In contrast, other angiogenic factors did not correlate with feeding artery dilatation, including the ratio of ang-2/ang-1, and tumor-feeding artery enlargement (p=0.115; Figure 3D left).

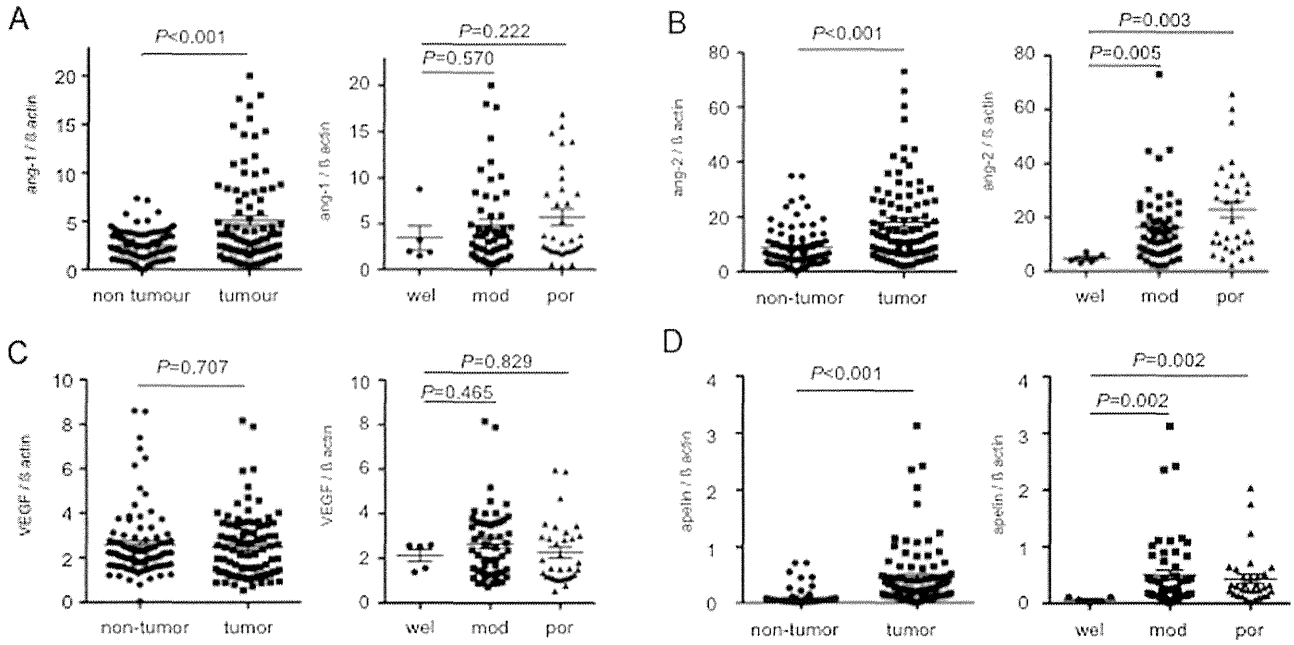

Figure 2. *qRT-PCR analysis of ang-1, ang-2, apelin and VEGF expression in clinical specimens. (A) Ang-1 expression was 2.1-fold higher in tumors than in normal liver tissues (p<0.001), but did not significantly differ between differentiation stages (B) Ang-2 expression was 2.1-fold higher in tumors than in normal liver tissue (p<0.001), and was expressed at higher levels in moderately- and poorly-differentiated tumors than in well-differentiated tumors (p=0.005, p=0.003, respectively). (C) VEGF expression did not significantly differ between tumor and non-tumor tissues or among differentiation stages. (D) Apelin expression was ~5.7-fold higher in tumor than in non-tumor tissues (p<0.001), and was higher in moderately- and poorly-differentiated tumors than in well-differentiated tumors (p=0.002, p=0.002).*

F13A inhibits tumor growth in a HCC subcutaneous tumor mouse model. To investigate the effect of antagonizing APJ *in vivo*, we generated HCC subcutaneous tumors by injection of MH134 cells into C3H mice. Treatment of mice with the APJ antagonist, F13A, led to significant inhibition of tumor growth compared to control mice (Figure 4A). Inhibition of tumor size was observed at day 7 post-injection of MH134 cells (p=0.007), and this difference continued until the end point. Pathological analysis of tumors was assessed 14 days after MH134 cell transplantation. Analysis of the percentage of necrotic tissue area by H&E staining revealed no difference between the F13A group (Figure 4C) and control (Figure 4B), despite tumors from control mice being significantly larger than those in F13A-treated mice (p=0.917; Figure 4D). MVD was examined by IHC for CD34 (Figure 5A). The MVD in F13A-treated mice was significantly less than in the control group (p=0.009; Figure 5B). We also examined AVD by IHC for caldesmon (Figure 5C). The AVD was also significantly less in F13A-treated mice (p=0.047; Figure 5D, left). Apelin acts not only as a neoangiogenic factor, but also dilates arteries (18); therefore, we assessed the number of arteries ≥10 μm in diameter. We observed a significant decrease in the number of arteries ≥10 μm in diameter in F13A-treated mice (p=0.008; Figure 5D, right). Taken together, these data indicate that F13A blocks both the apelinergic effects on neoangiogenesis and the dilation of arteries.

No significant differences in body weight and serum chemistry were observed in F13A-treated mice *versus* control mice (data not shown), and there were no obvious adverse effects associated with F13A treatment at the dose used (data not shown).

Discussion

HCC displays marked vascular abnormalities; aberrant microvasculature in the form of arteriogenesis and capillarization is typically observed (1, 5). Arteriogenesis is the growth of functional collateral arteries covered with smooth muscle cells from pre-existing arteries (4). Sinusoidal capillarization involves the transformation of fenestrated hepatic sinusoids into continuous capillaries, and is characterized by the expression of CD34, a marker absent in normal sinusoidal endothelium (1). As a result of these pathological changes, the hemodynamic status of HCC differs from that of non-tumorous liver (6). Whereas non-

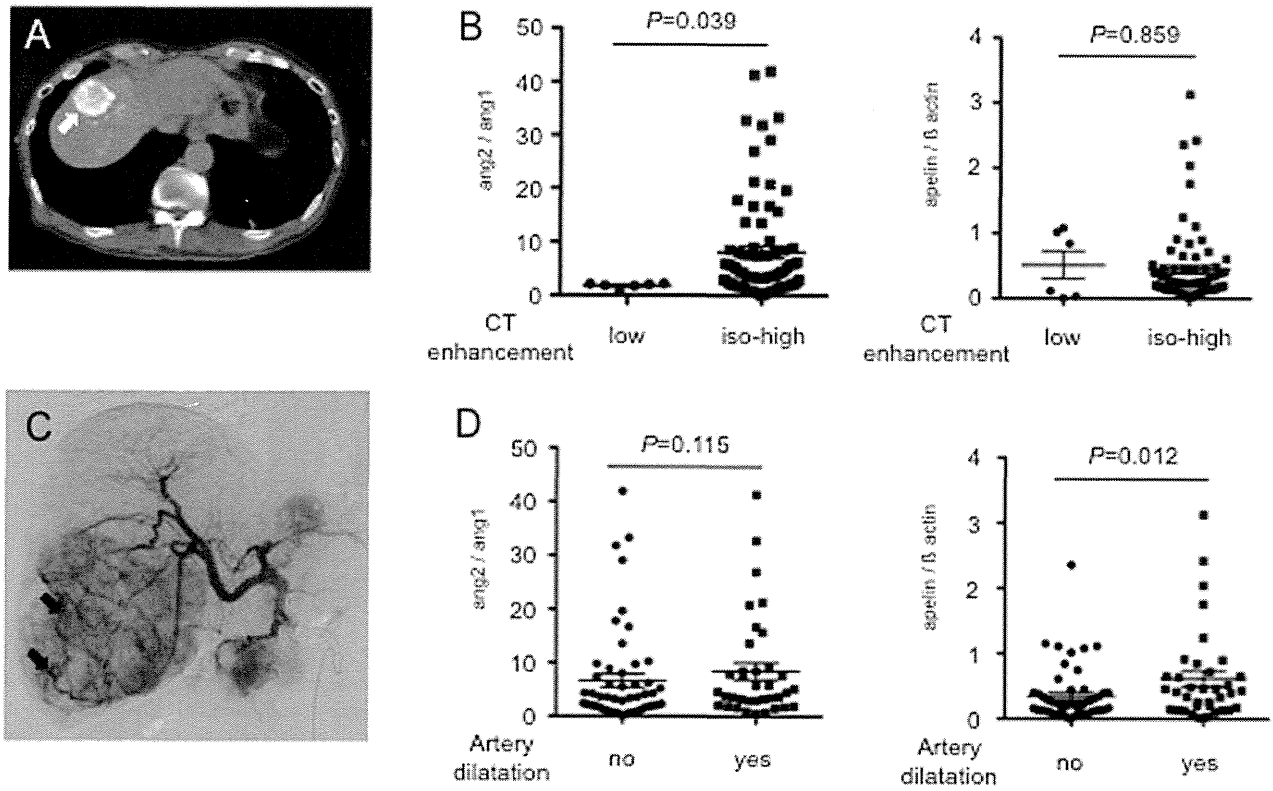

Figure 3. *Apelin is overexpressed in tumors with irregular dilation of feeding arteries. (A) HCC with CTHA enhancement. (B) Ang-2/ang-1 ratio was higher in tumors with positive CTHA enhancement (p=0.039). Apelin was not overexpressed in tumors with enhanced CTHA (p=0.859). (C) HCC with irregular dilatation of tumor feeding arteries on digital subtraction angiography. (D) Ang-2/ang-1 ratio did not correlated with tumors with irregular artery dilatation (p=0.115). Tumors with irregular dilatation of feeding arteries expressed higher levels of apelin than tumors without artery dilatation (p=0.012).*

tumorous liver has a dual supply of blood by arterial and portal flow, HCC receives arterial blood supply only (27).

In the present study, we used IHC to show that the apelin receptor, APJ, is expressed on arterial smooth muscle cells in HCC, and is overexpressed in HCC compared with non-tumorous tissue. *Apelin* mRNA was also overexpressed in HCC. Treatment with apelin is reported to increase the proliferation of smooth muscle cells (17). We observed a positive correlation between APJ and h-caldesmon$^+$ vessels especially in HCC tumor. These results suggest that the apelin-APJ system affects HCC arteriogenesis by promoting arterial smooth muscle cell proliferation. We also observed that tumors with irregular dilatation of feeding arteries expressed greater amounts of apelin than tumors without dilatation of the arteries. Apelin not only affects proangiogenesis, but also dilates vessels (14, 18). Both functions of apelin—dilating tumor-feeding arteries and promoting development of arterioles in HCC—are compatible with our result from clinical specimen. *In vivo*, treatment of HCC model mice with the APJ antagonist, F13A, significantly decreased AVD and the number of thick arteries. Tumor growth was also significantly decreased following F13A treatment. These results indicate that apelin-APJ affects HCC tumor growth *via* dilating tumor-feeding arteries and promoting development of arterioles.

Several angiogenic factors, including VEGF, ang-1 and ang-2, have been shown to regulate neovascularity in HCC (1, 9, 28), and reportedly affect vascular endothelial cells (29). Taken together, these reports imply that these angiogenic factors predominantly affect HCC capillarization. During arteriogenesis, proliferation of both smooth muscle cells and vascular endothelial cells are required to generate arterial structures. Therefore, other factors are required to develop vascular smooth muscle cells during arteriogenesis.

In a study of apelin hyperexpression in a subcutaneous colon cancer mouse model (30), enlargement and maturation of tumor vessels were seen in apelin-hyperexpressing tumor. Normalization of tumor vasculature helps combination antitumor therapies, because mature vasculature and increased blood flow to tumors can promote delivery of antitumor therapeutics to tumor cells. HCC is highly vascularized and is characterized by a high incidence of

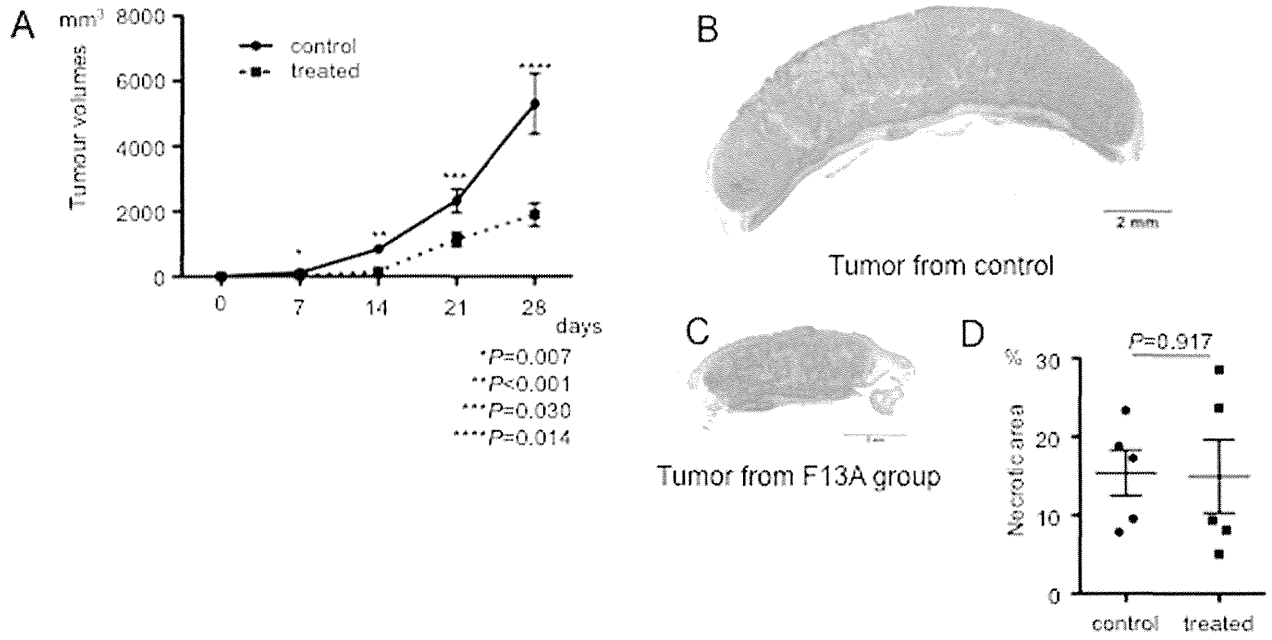

Figure 4. *Blocking apelin–APJ signaling with F13A inhibits tumor growth in an HCC subcutaneous murine tumor model. (A) Tumor growth was significantly inhibited in F13A-treated mice compared with controls (n=5 mice/group). (B) Control mouse tumor (H&E stain). (C) Tumor from an F13A-treated mouse (H&E stain). (D) Comparison of necrotic areas (H&E stain). No differences were observed between the two treatment groups, despite the smaller size of F13A-treated tumors.*

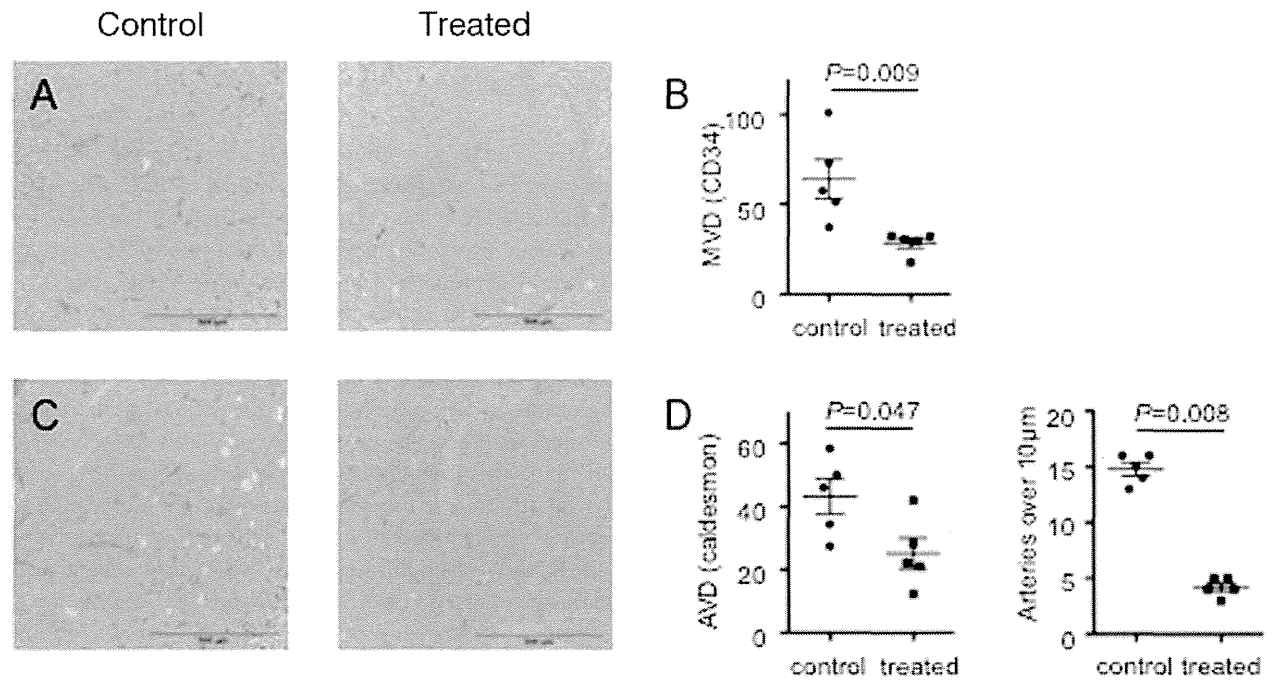

Figure 5. *Tumor vessel density is less in F13A-treated mice. (A) CD34 IHC staining of tumors from control mice (left) and F13A-treated mice (right). (B) MVD was significantly less in F13A-treated mice than in controls (p=0.009). (C) Caldesmon IHC staining of tumors from control mice (left) and F13A-treated mice (right). (D) AVD was significantly less in F13A-treated mice than in controls (p=0.047, left). The number of caldesmon$^+$ arteries (>10 μm in diameter) was significantly fewer in the F13A-treated group (p=0.008, right).*

AVD, not observed in other tumors, such as colon cancer (6). These characteristic high-density arterioles enable a supply of fresh arterial flow to the HCC and are reported to predict poor prognosis (31). These phenomena may suggest that mature arterioles may develop more frequently in HCC compared to other types of cancers, and that preventing angiogenesis could be a good therapeutic target in HCC. The difference in apelin production between colon cancer and HCC may account for the differences in arteriole density and differences underlying tumor growth.

In the present study, we have shown that Apelin-APJ is overexpressed, and can work as a signal for arteriogenesis in HCC. However, the mechanism by which APJ expression is specifically increased on smooth muscle cells of HCC tumors remains unclear. Further studies investigating the apelinergic system in HCC are required.

Disclosure

This work was supported in part by grants-in-aid from the Japan Ministry of Education, Culture, Sports, Science and Technology (24592005).

Financial Support

This work was supported in part by grants-in-aid from the Japan Ministry of Education, Culture, Sports, Science and Technology (24592005).

Conflicts of Interest

The Authors have no conflicts of interest.

Acknowledgements

The authors would like to thank Prof. Hiroshi Honda, Department of Clinical Radiology and Prof. Yoshinao Oda, Department of Anatomic Pathology, Pathological Science, Graduate School of Medical Sciences, Kyushu University, for advice and discussions. The authors would also like to thank Ms. T Shishino, Ms. N Makikusa, Ms. M Kiyota, Ms. K Misumi, Ms. Y Kubota and Ms. M Nakajima for their excellent technical assistance.

References

1 Zhu AX, Duda DG, Sahani DV and Jain RK: HCC and angiogenesis: possible targets and future directions. Nat Rev Clin Oncol *8*: 292-301, 2011.

2 Sonoda T, Shirabe K, Takenaka K, Kanematsu T, Yasumori K and Sugimachi K: Angiographically undetected small hepatocellular carcinoma: clinicopathological characteristics, follow-up and treatment. Hepatology *10*: 1003-1007, 1989.

3 Tanigawa N, Lu C, Mitsui T and Miura S: Quantitation of sinusoid-like vessels in hepatocellular carcinoma: its clinical and prognostic significance. Hepatology *26*: 1216-1223, 1997.

4 Carr BI: Hepatocellular carcinoma: current management and future trends. Gastroenterology *127*: S218-224, 2004.

5 Muto J, Shirabe K, Sugimachi K and Maehara Y: Review of angiogenesis in hepatocellular carcinoma. Hepatology research : the official journal of the Japan Society of Hepatology 2014.

6 Matsui O, Kobayashi S, Sanada J, Kouda W, Ryu Y, Kozaka K, Kitao A, Nakamura K and Gabata T: Hepatocelluar nodules in liver cirrhosis: hemodynamic evaluation (angiography-assisted CT) with special reference to multi-step hepatocarcinogenesis. Abdom Imaging *36*: 264-272, 2011.

7 Zhu AX: Systemic treatment of hepatocellular carcinoma: dawn of a new era? Ann Surg Oncol *17*: 1247-1256, 2010.

8 Sugimachi K, Tanaka S, Taguchi K, Aishima S, Shimada M and Tsuneyoshi M: Angiopoietin switching regulates angiogenesis and progression of human hepatocellular carcinoma. J Clin Pathol *56*: 854-860, 2003.

9 Mitsuhashi N, Shimizu H, Ohtsuka M, Wakabayashi Y, Ito H, Kimura F, Yoshidome H, Kato A, Nukui Y and Miyazaki M: Angiopoietins and Tie-2 expression in angiogenesis and proliferation of human hepatocellular carcinoma. Hepatology *37*: 1105-1113, 2003.

10 Yang XR, Xu Y, Yu B, Zhou J, Qiu SJ, Shi GM, Zhang BH, Wu WZ, Shi YH, Wu B, Yang GH, Ji Y and Fan J: High expression levels of putative hepatic stem/progenitor cell biomarkers related to tumour angiogenesis and poor prognosis of hepatocellular carcinoma. Gut *59*: 953-962, 2010.

11 O'Dowd BF, Heiber M, Chan A, Heng HH, Tsui LC, Kennedy JL, Shi X, Petronis A, George SR and Nguyen T: A human gene that shows identity with the gene encoding the angiotensin receptor is located on chromosome 11. Gene *136*: 355-360, 1993.

12 Tatemoto K, Hosoya M, Habata Y, Fujii R, Kakegawa T, Zou MX, Kawamata Y, Fukusumi S, Hinuma S, Kitada C, Kurokawa T, Onda H and Fujino M: Isolation and characterization of a novel endogenous peptide ligand for the human APJ receptor. Biochem Biophys Res Commun *251*: 471-476, 1998.

13 Eyries M, Siegfried G, Ciumas M, Montagne K, Agrapart M, Lebrin F and Soubrier F: Hypoxia-induced apelin expression regulates endothelial cell proliferation and regenerative angiogenesis. Circ Res *103*: 432-440, 2008.

14 Kidoya H, Ueno M, Yamada Y, Mochizuki N, Nakata M, Yano T, Fujii R and Takakura N: Spatial and temporal role of the apelin/APJ system in the caliber size regulation of blood vessels during angiogenesis. EMBO J *27*: 522-534, 2008.

15 Dai T, Ramirez-Correa G and Gao WD: Apelin increases contractility in failing cardiac muscle. Eur J Pharmacol *553*: 222-228, 2006.

16 Zhong JC, Huang DY, Liu GF, Jin HY, Yang YM, Li YF, Song XH and Du K: Effects of all-trans retinoic acid on orphan receptor APJ signaling in spontaneously hypertensive rats. Cardiovasc Res *65*: 743-750, 2005.

17 Cui RR, Mao DA, Yi L, Wang C, Zhang XX, Xie H, Wu XP, Liao XB, Zhou H, Meng JC, Yuan LQ and Liao EY: Apelin suppresses apoptosis of human vascular smooth muscle cells *via* APJ/PI3-K/Akt signaling pathways. Amino Acids *39*: 1193-1200, 2010.

18 Hashimoto T, Kihara M, Ishida J, Imai N, Yoshida S, Toya Y, Fukamizu A, Kitamura H and Umemura S: Apelin stimulates myosin light chain phosphorylation in vascular smooth muscle cells. Arterioscler Thromb Vasc Biol *26*: 1267-1272, 2006.

19 Kidoya H, Naito H and Takakura N: Apelin induces enlarged and nonleaky blood vessels for functional recovery from ischemia. Blood *115*: 3166-3174, 2010.

20 Berta J, Kenessey I, Dobos J, Tovari J, Klepetko W, Jan Ankersmit H, Hegedus B, Renyi-Vamos F, Varga J, Lorincz Z, Paku S, Ostoros G, Rozsas A, Timar J and Dome B: Apelin expression in human non-small cell lung cancer: role in angiogenesis and prognosis. J Thorac Oncol *5*: 1120-1129, 2010.

21 Heo K, Kim YH, Sung HJ, Li HY, Yoo CW, Kim JY, Park JY, Lee UL, Nam BH, Kim EO, Kim SY, Lee SH, Park JB and Choi SW: Hypoxia-induced up-regulation of apelin is associated with a poor prognosis in oral squamous cell carcinoma patients. Oral Oncol 2012.

22 Wang Z, Greeley GH Jr. and Qiu S: Immunohistochemical localization of apelin in human normal breast and breast carcinoma. J Mol Histol *39*: 121-124, 2008.

23 Sorli SC, van den Berghe L, Masri B, Knibiehler B and Audigier Y: Therapeutic potential of interfering with apelin signalling. Drug Discov Today *11*: 1100-1106, 2006.

24 Sorli SC, Le Gonidec S, Knibiehler B and Audigier Y: Apelin is a potent activator of tumour neoangiogenesis. Oncogene *26*: 7692-7699, 2007.

25 Kayashima H, Toshima T, Okano S, Taketomi A, Harada N, Yamashita Y, Tomita Y, Shirabe K and Maehara Y: Intratumoral neoadjuvant immunotherapy using IL-12 and dendritic cells is an effective strategy to control recurrence of murine hepatocellular carcinoma in immunosuppressed mice. J Immunol *185*: 698-708, 2010.

26 Fujita N, Aishima S, Iguchi T, Nishihara Y, Yamamoto H, Taketomi A, Oda Y, Honda H and Tsuneyoshi M: Down-regulation of artery in moderately differentiated hepatocellular carcinoma related to tumor development. Hum Pathol *41*: 838-847, 2010.

27 Kim HC, Kim TK, Sung KB, Yoon HK, Kim PN, Ha HK, Kim AY, Kim HJ and Lee MG: CT during hepatic arteriography and portography: an illustrative review. Radiographics *22*: 1041-1051, 2002.

28 Park YN, Kim YB, Yang KM, Park C. Increased expression of vascular endothelial growth factor and angiogenesis in the early stage of multistep hepatocarcinogenesis. Arch Pathol Lab Med *124*: 1061-1065, 2000.

29 Mazzieri R, Pucci F, Moi D, Zonari E, Ranghetti A, Berti A, Politi LS, Gentner B, Brown JL, Naldini L and De Palma M: Targeting the ANG2/TIE2 axis inhibits tumor growth and metastasis by impairing angiogenesis and disabling rebounds of proangiogenic myeloid cells. Cancer Cell *19*: 512-526, 2011.

30 Kidoya H, Kunii N, Naito H, Muramatsu F, Okamoto Y, Nakayama T and Takakura N: The apelin/APJ system induces maturation of the tumor vasculature and improves the efficiency of immune therapy. Oncogene 2011.

31 Zhang ZB, Cai L, Zheng SG, Xiong Y and Dong JH: Overexpression of caveolin-1 in hepatocellular carcinoma with metastasis and worse prognosis: correlation with vascular endothelial growth factor, microvessel density and unpaired artery. Pathology oncology research: POR *15*: 495-502, 2009.

Received June 28, 2014
Accepted July 16, 2014

Use of Living Donor Liver Grafts With Double or Triple Arteries

Hideaki Uchiyama,[1,2] Ken Shirabe,[1] Tomoharu Yoshizumi,[1] Toru Ikegami,[1] Yuji Soejima,[1] Yoichi Yamashita,[1] Hirofumi Kawanaka,[1] Tetsuo Ikeda,[1] Masaru Morita,[1] Eiji Oki,[1] and Yoshihiko Maehara[1]

Background. Hepatic grafts used in living donor liver transplantation (LDLT) sometimes have two or more arteries, in which surgeons are required to perform complex arterial reconstruction. The aim of the current study was to demonstrate whether selecting living donor liver grafts with double or triple arteries yielded the same outcomes as grafts with a single artery.

Methods. We retrospectively investigated the outcomes of LDLT focusing on the numbers of arteries on grafts. Four hundred forty-six cases of LDLT performed between October 1996 and October 2012 were retrospectively analyzed. The cases were divided into the following three groups according to the number of arteries on a graft: the single (n=331), the double (n=108), and the triple (n=7) groups.

Results. Artery-related complications occurred in five cases in the single group, two cases in the double group, and no case in the triple group. Although the overall graft survival was comparable among the three groups, there was a tendency of worsened graft survival and increased incidence of anastomotic biliary stricture after liver transplantation in right hepatic grafts with double arteries.

Conclusions. The use of grafts with double or triple arteries yielded favorable outcomes with minimum artery-related complications compared with grafts with a single artery. However, the use of right hepatic grafts with double arteries is discouraging in the current study.

Keywords: Hepatic artery reconstruction, Living donor liver transplantation, Microvascular surgery.

(*Transplantation* 2014;97: 1172–1177)

Despite the recent advancements in surgical techniques in living donor liver transplantation (LDLT), hepatic artery reconstruction still remains to be one of the most difficult procedures in LDLT because arteries on grafts to be reconstructed are relatively thin and short compared with deceased liver transplantation (*1–4*). Preoperative evaluations for candidate donors in LDLT sometimes reveal that a hepatic graft will have two or more arteries (*4*). These arteries are usually thinner and shorter compared with single arteries, which makes arterial reconstruction much more difficult (*3, 5–7*). Furthermore, the use of such grafts requires surgeons to perform complex arterial reconstruction or compromise with incomplete reconstruction, that is, abandon reconstructing all graft arteries. Selective arterial reperfusion may result in relative arterial ischemia in the graft leading to biliary complication, such as biliary stricture or cholangitis (*3*).

We had attempted to reconstruct all graft arteries since the implementation of our LDLT program if technically feasible (*4*). It remains to be elucidated whether the use of such grafts yields the same outcomes, as grafts with a single artery. If selecting hepatic grafts, which would have two or three arteries, might affect the outcomes of LDLT, such grafts would have a lower priority than grafts with a single artery. Therefore, we retrospectively investigated the outcomes of LDLT using grafts with double or triple arteries.

RESULTS

Operative Results of Living Donor Liver Transplantation According to the Number of Arteries on Grafts

Table 1 summarizes the numbers of arteries on a graft and the numbers of reconstructed arteries. Ninety-four of the 262 left grafts had two arteries, and both arteries were

The authors declare no funding or conflicts of interest.

[1] Department of Surgery and Science, Graduate School of Medical Sciences, Kyushu University, Fukuoka, Japan.

[2] Address correspondence to: Hideaki Uchiyama, Department of Surgery and Science, Graduate School of Medical Sciences, Kyushu, University, Fukuoka, 812-8582, Japan.

E-mail: huchi@surg2.med.kyushu-u.ac.jp

All the other authors except the first author equally participated in the performance of the research and data analysis, and the first author (H.U.) participated in research design, writing of this manuscript, performance of the research, and data analysis.

Supplemental digital content (SDC) is available for this article. Direct URL citations appear in the printed text, and links to the digital files are provided in the HTML text of this article on the journal's Web site (www.transplantjournal.com).

Received 24 September 2013. Revision requested 8 October 2013.
Accepted 15 November 2013.

ISSN: 0041-1337/14/9711-1172
DOI: 10.1097/01.TP.0000442687.33536.c4

TABLE 1. Summary of the number of arteries on the graft and the number of reconstructed arteries

Graft type	No. of hepatic arteries	n	No. of the reconstructed arteries	n
Left	One artery	161	One reconstruction	161
	Two arteries	94	One reconstruction	32
			Two reconstructions	62
	Three arteries	7	One reconstruction	1
			Two reconstructions	3
			Three reconstructions	3
Right	One artery	133	One reconstruction	133
	Two arteries	8	One reconstruction	0
			Two reconstructions	8
Lateral	One artery	31	One reconstruction	31
			One reconstruction	3
	Two arteries	6	Two reconstruction	3
Posterior	One artery	6	One reconstruction	6

reconstructed in 62 grafts (66%). Seven left grafts had three arteries, and two of the three arteries were reconstructed in three grafts (43%), and all the three arteries were reconstructed in three grafts (43%). Eight of 141 right grafts had two arteries, and both arteries were reconstructed in all the eight grafts (100%). Six of the 37 left lateral grafts had two arteries, and both arteries were reconstructed in three grafts (50%).

The patient characteristics and operative results considering all types of liver grafts (left grafts, right grafts, left lateral grafts, and posterior grafts) are summarized comparing each factor among the three groups (see **Table S1, SDC,** http://links.lww.com/TP/A925). The grafts from male donors had a tendency to have multi-arteries compared with the grafts from female donors. The mean outer diameter of the reconstructed graft arteries in the double group (2.35±0.06 mm) was significantly thinner than that in the single group (2.82±0.04 mm). Furthermore, the diameter of graft arteries in the triple group (1.88±0.18 mm) was thinner than the double group ($P<0.01$). Although the more arteries liver grafts had the longer the operation times, the factor did not reach statistical significance. Five and two hepatic artery complications were observed in the single group and the double group, respectively, whereas there was no hepatic artery complication in the triple group.

The patient characteristics and operative results considering only left grafts are summarized comparing each factor among the three groups (see **Table S2, SDC,** http://links.lww.com/TP/A925). The grafts from the male donors had a tendency to have double and triple arteries compared with the grafts from female donors. The mean outer diameter of the reconstructed graft arteries in the double group (2.39±0.07 mm) was significantly thinner than that in the single group (2.79±0.06 mm). Furthermore, the diameter of graft arteries in the triple group (1.88±0.18 mm) was thinner than the double group ($P<0.01$). The more hepatic arteries liver graft had, the longer the operation time. The increase of intraoperative blood loss was observed in the double and the triple groups, although there was no statistical significance. Artery-related complications were observed in three cases (two hepatic artery thromboses and one aneurysm formation) in the single group and in one case (pseudoaneurysm formation) in the double group.

The patient characteristics and operative results considering only right grafts are summarized comparing each factor between the two groups (see **Table S3, SDC,** http://links.lww.com/TP/A925). The mean of the reconstructed arterial diameters was significantly thinner in the double group (2.32±0.19 vs. 2.96±0.06 mm) ($P<0.01$). However, the mean operative times and the mean intraoperative blood losses were comparable between the single and the double group. Artery-related complications were observed in two cases (hepatic artery dissection and inflow insufficiency) in the single group and one case (hepatic artery dissection) in the double group.

The patient characteristics and operative results considering only left lateral grafts are summarized comparing each factor among the three groups (see **Table S4, SDC,** http://links.lww.com/TP/A925).

The mean of the reconstructed arterial diameters in the double group (1.75±0.19 mm) was significantly thinner than that in the single group (2.42±0.11 mm) ($P<0.01$). The mean operation time in the double group was significantly longer than that in the single group. There was more blood loss in the double group than in the single group. There was no hepatic artery complication in LDLT using left lateral grafts.

The seven hepatic artery complications were summarized in Table S5 (see **SDC,** http://links.lww.com/TP/A925).

Graft Survival According to the Number of Hepatic Arteries on a Graft

Figure 1 shows the comparisons of the graft survival in each group. The survival curves of left grafts, right grafts, and left lateral grafts were individually compared (Fig. 1B–D), which revealed there were no significant difference among the single, double, and triple groups when considering the all grafts (Fig. 1A), when considering only left grafts (Fig. 1B), and when considering only left lateral grafts (Fig. 1D). There was a tendency to worse graft survival in the double group. However, it did not reach statistical significance ($P=0.11$) (Fig. 1C).

Incidence of Anastomotic Biliary Stricture According to the Number of Hepatic Arteries on a Graft

Arterial ischemia is thought to be one of the main causes for anastomotic biliary stricture after living donor liver transplantation (*3*). As shown in Figure 2, there were no significant difference among the single, the double, and the triple groups when considering all grafts (left grafts, right grafts, left lateral grafts, and posterior grafts) (Fig. 2A), when considering only left grafts (Fig. 2B), and when considering only left lateral grafts (Fig. 2D). However, there was a statistically significant difference between the single and the double groups when considering only right grafts ($P=0.02$) (Fig. 2C).

DISCUSSION

The major disadvantages in the use of living donor liver grafts are anatomic complexities and small graft volumes

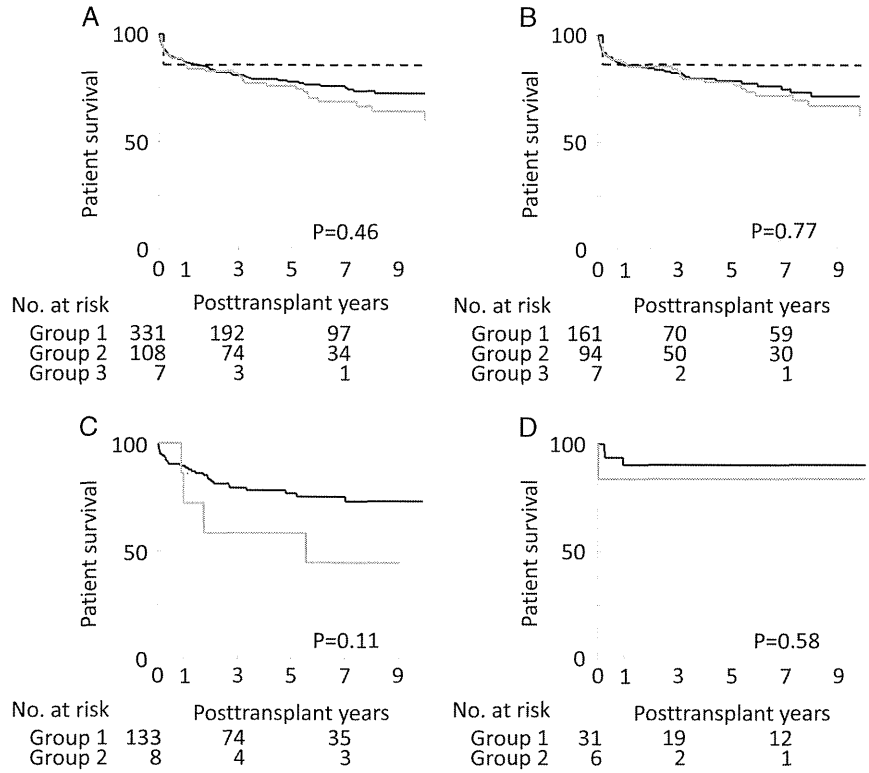

FIGURE 1. Graft survival after living donor liver transplantation according to the number of arteries on the grafts: (A) considering all grafts (left grafts, right grafts, left lateral grafts, and posterior grafts), (B) considering only left grafts, (C) considering only right grafts, and (D) considering only left lateral grafts. Solid black line, the single group; solid gray line, the double group; dotted black line, the triple group.

(*8–10*). The anatomic diversity of the hepatic arteries sometimes causes difficulty in reconstructing graft hepatic arteries. In our experience, approximately one third of hepatic grafts in LDLT had two or three hepatic arteries as shown in Table 1. Especially, approximately 40 % of left grafts had two or three arteries. The more arteries a hepatic graft had, the more technically demanding the hepatic artery reconstruction was. In our initial experience, a candidate left graft, which was expected to have triple arteries, was not selected because of the complexity of hepatic artery reconstruction. However, with cumulative experience, we have accustomed to reconstruct thin and tiny graft hepatic arteries. As a result, a graft with triple arteries have no longer been considered as a contraindication and have yielded comparable outcomes as observed in using hepatic grafts with a single artery. Microvascular surgical technique broadened the selection of hepatic grafts, which may increase the safety of living liver donors, that is, we can preferentially select left grafts (*11, 12*). If two candidate donors, one for a left lobe graft with triple arteries and another for a right lobe graft with a single artery, are available, we will select the donor for a left lobe graft, although longer operation time and increased blood loss are expected. Nonetheless, recipient hepatic arteries should be divided as peripherally as possible to make candidate recipient inflow arteries for reconstructing tiny graft hepatic arteries, which needed longer operation time as evidenced in the current study.

The question of whether all hepatic arteries on a graft have to be reconstructed is still a matter for debate. Some surgeons reported only one hepatic artery reconstruction would suffice in most cases because there are sufficient intrahepatic arterial networks (*5, 13, 14*). There is usually a pulsatile backflow from the other artery after the first graft artery have been reconstructed, which suggests there are sufficient intrahepatic arterial networks, and the second arterial reconstruction is not necessarily mandatory. However, how do we define the adequate strength of the backflow at which level we can safely abandon the second arterial reconstruction? The decision about whether the second arterial reconstruction should be performed is apparently subjective. Surgeons cannot quantify it at the present time. When the left hepatic artery nourishes segments 2 and 3 and the middle hepatic artery nourishes the segment 4, only a reconstruction of the left hepatic artery will result in arterial ischemia in segment 4 unless there are sufficient intrahepatic arterial networks between the segment 2/3 and 4. We previously reported only one hepatic artery reconstruction resulted in the increased incidence of anastomotic biliary stricture presumably because of relative arterial ischemia in hepatic grafts (*3*). Furthermore, we experienced an infarcted medial segment probably caused by not reconstructing the middle hepatic artery (unpublished data). With the aforementioned experience, we have tried to reconstruct all arteries on a hepatic graft even if the effort was time consuming. The decision about whether the second hepatic artery

needs to be reconstructed should be objective. With cumulative experience, we have become capable of safely reconstructing almost all hepatic arteries. We strongly advocate that all hepatic arteries should be reconstructed if technically feasible because there is no objective measure to decide whether the second or the third hepatic artery reconstruction is necessary.

Some authors reported manipulation of donors' hepatic artery to simply reconstruct graft hepatic arteries (*6, 7*). However, the safety of living liver donors is of paramount importance. Surgical interventions to living donors should be as minimal as possible. If a surgeon is capable of safely reconstructing multiple arteries on hepatic grafts, there is no need for additional intervention to donors whose liver graft will expect to have two or more arteries.

One presumed reason why right grafts with double arteries had a poorer graft survival and a high incidence of anastomotic biliary stricture is that a right graft with double arteries often has anatomic anomalies of the portal branches and the hepatic ducts. We identified a significant correlation between the number of arteries and the number of portal veins. Three of eight grafts with double arteries had two portal veins (the anterior branch of the right portal vein and the posterior branch of the right portal vein), whereas only three of 133 grafts with a single artery had two portal veins. Liver transplants using grafts with not only double hepatic arteries but also double portal veins were extremely complex procedure, which might explain the worse graft survival in patients who received a right graft with double arteries. There was no significant correlation between the number of arteries and the number of bile duct orifices. The presumed reason why the incidence of biliary stricture was high in patients who received a right graft with double arteries was that recipient hepatic arteries had to be extensively isolated in order to reconstruct both two arteries, which resulted in disruption of tiny nourishing arteries into the bile duct, leading to the bile duct ischemia.

The introduction of microvascular surgery to hepatic artery reconstruction was one of the greatest innovations in LDLT (*15–17*). We introduced microvascular surgery to hepatic artery reconstruction in LDLT in the beginning of our LDLT program and almost all hepatic artery reconstructions were done under a microscope. Mastering reconstructing hepatic arteries under a microscope is time-consuming for many reasons. First, there are constant movements of the operative field caused by heart beats and respiration. Second, the operative field is deep in the abdominal cavity, which needs long forceps and a needle holder. Third, there are a lot of embarrassing collateral vessels around candidate recipient inflow arteries, which makes isolation of these arteries difficult. However, once a surgeon masters the procedure, almost all graft hepatic arteries can be reconstructed as long as there is a recipient inflow artery.

In conclusion, the presence of double or triple hepatic arteries on a hepatic graft did not necessarily increase the

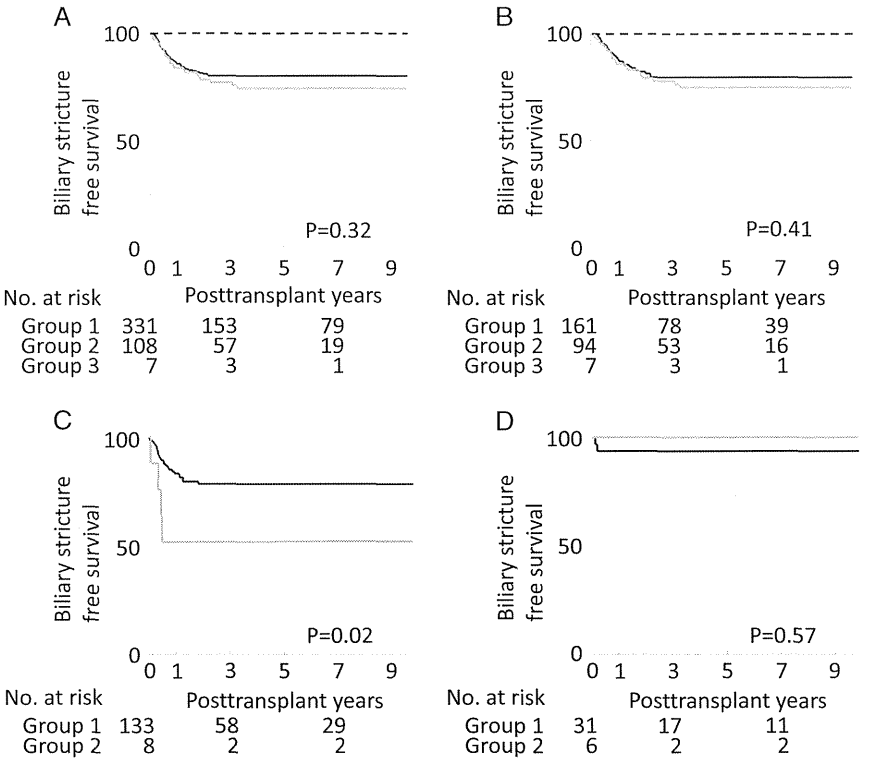

FIGURE 2. Biliary stricture-free survival after living donor liver transplantation according to the number of arteries on the grafts: (A) considering all grafts (left grafts, right grafts, left lateral grafts, and posterior grafts), (B) considering only left grafts, (C) considering only right grafts, and (D) considering only left lateral grafts. Solid black line, the single group; solid gray line, the double group; dotted black line, the triple group.

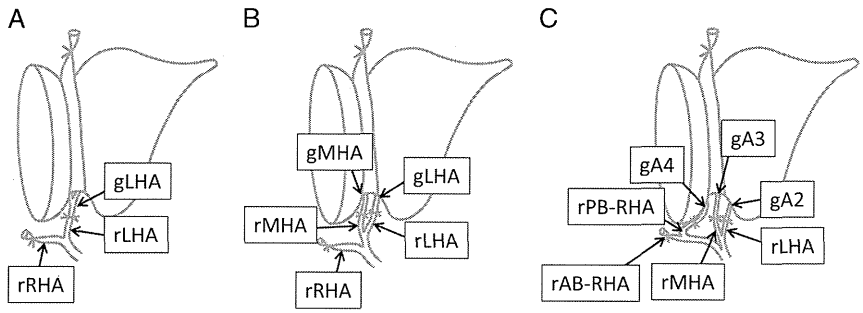

FIGURE 3. Representative schematic diagrams of hepatic arterial reconstruction using (A) a graft with a single artery and (B) a graft with double arteries and (C) a graft with triple arteries. gA2, graft hepatic artery into the segment 2; gA3, graft hepatic artery into the segment 3; gA4, graft hepatic artery into the segment 4; gLHA, graft left hepatic artery; gMHA, graft middle hepatic artery; rAB-RHA, recipient anterior branch of the right hepatic artery; rLHA, recipient left hepatic artery; rMHA, recipient middle hepatic artery; rPB-RHA, recipient posterior branch of the right hepatic artery; rRHA, recipient right hepatic artery.

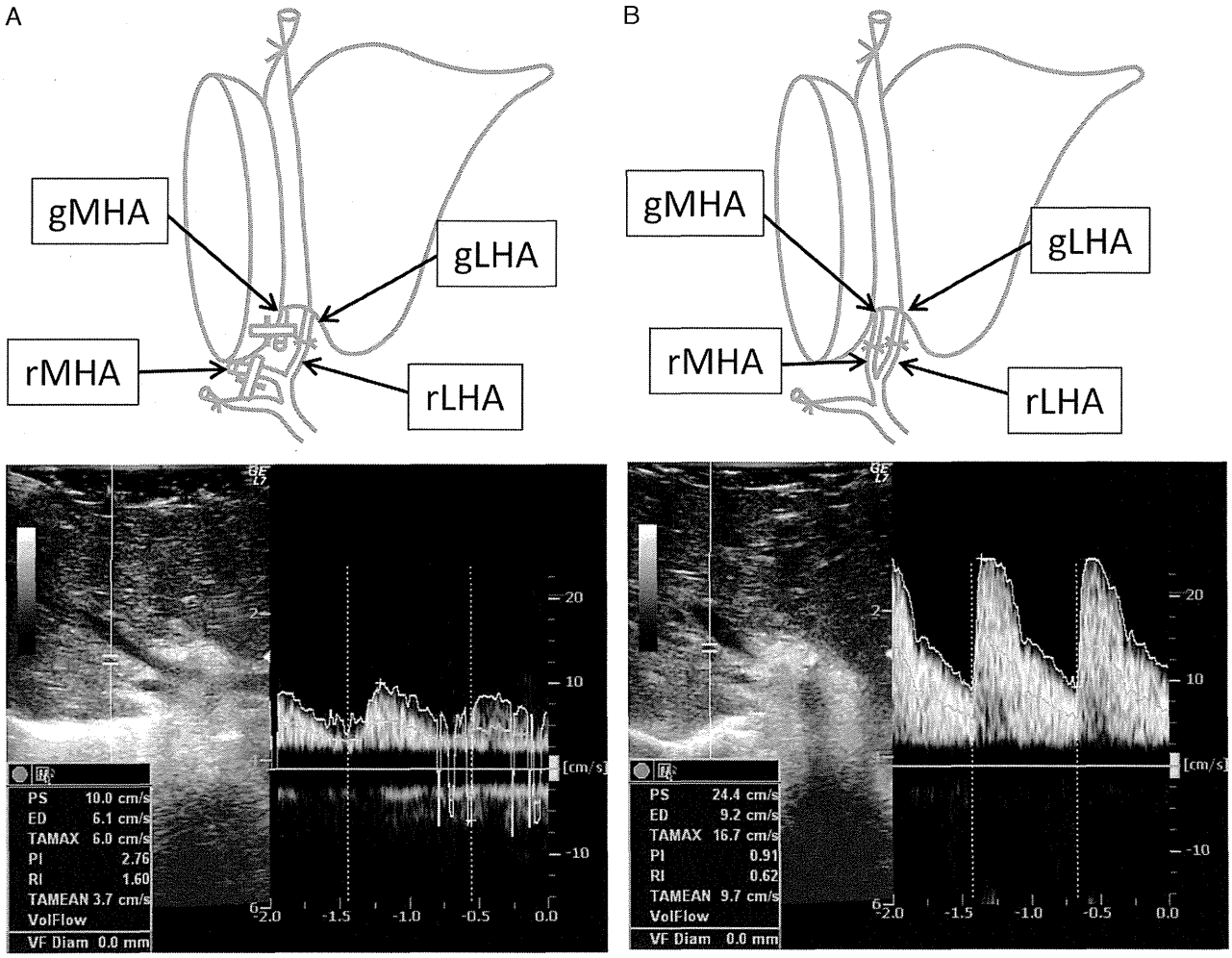

FIGURE 4. Doppler sonography (A) after only the left hepatic artery was reconstructed and (B) after the middle hepatic artery was also reconstructed. Only weak pulsatile arterial flow in the segment 4 was recognized when only the left hepatic artery was reconstructed. After the middle hepatic artery was reconstructed, the pulsatile arterial flow in the segment 4 became stronger. gLHA, graft left hepatic artery; gMHA, graft middle hepatic artery; rLHA, recipient left hepatic artery; rMHA, recipient middle hepatic artery.